Influence of Alkyl Chain Spacer Length on the Charge Carrier Mobility of Isotactic Poly (*N*-carbazolylalkyl acrylates)

Sanket Samal, and Barry C. Thompson*

Department of Chemistry, Loker Hydrocarbon Research Institute, University of Southern California, Los Angeles, California 90089-1661, United States

ABSTRACT: In the search for semiconducting polymer alternatives to conjugated polymers, stereoregular non-conjugated pendant electroactive polymers (NCPEPs) have recently shown competitive hole mobilities with conjugated polymers and a dramatic increase in mobility relative to atactic analogues. Here we investigate one of the key structural variables of NCPEPs: the flexible alkyl spacer that separates the electroactive pendant from the backbone. We investigate a straightforward post-polymerization functionalization synthetic method to synthesize such polymers with high isotacticity using poly (*N*-carbazoylalkyl acrylate) as model system, where the alkyl chain spacer in the NCPEPs is varied from 2 to 12 carbons. We observed that the hole mobility increased from the 2-carbon spacer, resulting in the highest mobility upon thermal annealing with a 4-carbon spacer for 75% isotactic polymers and with a 6-carbon spacer for 87% isotactic polymers. As such, we have demonstrated an important role of the spacer chain in influencing mobility. For all spacer lengths, higher mobilities were measured with the more isotactic polymer. While physical characterization of the largely amorphous polymers yielded little insight into the structure-function relationships, DFT and MD simulations indicated helical structures for the polymers where intermolecular short range π-stacking is observed and is affected by spacer chain length. This work demonstrates that both degree of stereoregularity and spacer chain length play a role in determining the hole mobility in NCPEPs.

Conjugated polymers (CPs) are appealing for many electronic applications,[1,2] including organic light emitting diodes (OLEDs),[3] organic photovoltaics (OPVs),[4] organic field effect transistors (OFETs),[5] batteries,[6] and bioelectronics[7] due to their optical, semiconducting, biocompatibility and electrochemical properties. CPs also have numerous advantages over inorganic analogues such as lightweight, low-cost, flexibility, low toxicity and compatibility with roll-to-roll processing.[8] In recent years optimized polymers have led to high performance devices.[9–12]

However, CPs do suffer from several deficiencies including poor environmental stability,[13] limited mechanical properties,[14] low molecular weights,[15] and limited synthetic methodologies to achieve advanced architectures. While there have been advancements towards achieving CPs with controlled polymerizations;[16] it is still challenging to synthesize polymers with narrow dispersity (*Đ*), high molecular weight, and control over end groups.[17,18,19,20]

Non-conjugated electroactive polymers have garnered interest over the years due to the limitations of CPs.[21,22] Studies have shown that non-conjugated polymers containing electroactive pendant groups, also called non-conjugated pendant electroactive polymers (NCPEPs), possess enormous potential. In analogy to side chain liquid crystal polymers (SCLCPs),[23,24] it is expected that the properties of these polymers will be strongly influenced by the structure of the main chain, pendant group, spacer chain, and stereoregularity (Figure 1).[25,26] NCPEPs are attractive because of their easy pendant modification, high achievable molecular weights, diversity in accessible synthetic methodologies and the potential for precise control over hierarchical assemblies enabled by advanced architectures. Due to these strengths, they have been explored for use in organic electronics, notably in the work of Thelakkat.[27–29]

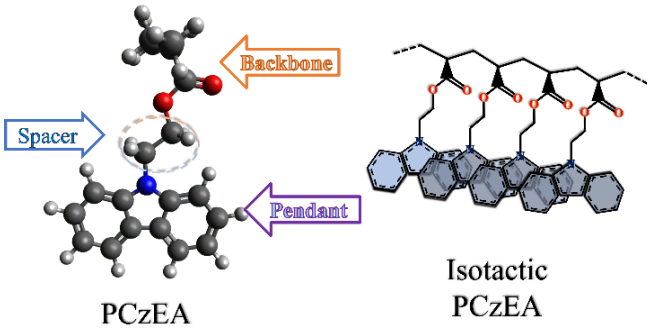

Figure 1. Structure of the NCPEP poly(2-*N*-carbazoylethyl acrylate (PCzEA) indicating the structural variables (left) and an isotactic polymer PCzEA (right).

NCPEPs are also of potential interest in flexible electronics due to analogy with insulating polymers (e.g., HDPE) that have been demonstrated to improve mechanical properties in polymer and polymer/fullerene blends.[30,31] Despite such potential advantages, NCPEPs are generally reported to have charge carrier mobilities several orders of magnitude lower than CPs.[32]

Inspired by Uryu *et al.*,[33] who showed that highly isotactic poly(2-*N*-carbazoylethyl acrylate) (PCzEA) (Figure 1) had a hole mobility (μ_h) six times higher than the atactic counterpart and the theoretical proposition of improvement in μ_h with increased backbone stereoregularity of poly(*N*-vinylcarbazole) (PVK);[34,35] we have recently shown clear evidence of the monotonic increase in μ_h with increasing isotacticity in PCzEA. We found that μ_h increased from 2.11 x 10^{-6} cm^2 V^{-1} s^{-1} to 4.68 x 10^{-5} cm^2 V^{-1} s^{-1} in unannealed samples as the dyad isotacticity increased from ~45% to ~95%, and μ_h is enhanced

to 2.74 x 10^{-4} cm^2 V^{-1} s^{-1} with thermal annealing of the 95% isotactic sample, rivalling poly(3-hexylthiophene) (P3HT).[36] Later work has shown that μ_h was increased with tacticity for PVK.[37]

However, there are several structural variables that can potentially influence μ_h, including the main chain, pendant group, spacer, and stereoregularity,[38,39]and understanding the structure-function relationships is essential for designing higher performing polymers. In our previous report on PCzEA, the alkyl spacer was kept constant at two carbons and only the effect of stereoregularity on μ_h was studied. Here we investigate for the first time the role of spacer length on charge-carrier mobility in stereoregular electroactive pendant polymers.

Hence, we report the synthesis of a family of poly(*N*-carbazoylalkyl acrylate) (PCzXA) polymers with different even number alkyl spacers ranging from two to twelve carbons. We investigate these spacers on two different isotactic PCzXAs of ~75% and ~87% dyad isotacticty. We find that as the spacer length increases from two carbons to either four or six carbons, the μ_h increases. With spacers longer than six carbons, the effect of the isotacticity is diminished as the degrees of freedom are increased and the μ_h decreases.

Although odd-even effects have been observed for thermal and physical properties with SCLCPs[24,40] we have limited our work to even spacers. In our previous work we used direct polymerization of *N*-carbazoylethyl acrylate and found that anionic polymerization gave the highest isotacticity. Anionic polymerization was preferred as it gives high stereocontrol under living polymerization conditions, which is important for extension to advanced architectures.[41] However anionic polymerization can pose a limitation due to functional group tolerance. Hence, here we explored post-polymerization functionalization with transesterification of acrylates, which has been shown to be quantitative under several conditions.[42–44] Another advantage of post-polymerization functionalization is that it allows an "apples-to-apples" comparison as one can examine a structural variable on otherwise identical backbones.

We did however attempt the direct polymerization route. The direct synthetic route is depicted in Scheme **S1** (Supporting Information). Synthesis of the 2-C acrylate, was achieved according to the literature.[45] Monomers with four, six and eight carbon spacers were also synthesized. Monomers were polymerized using *n*-BuLi in toluene. While the polymers gave reasonable dyad isotacticities of ~80%, the molecular weights were low, ranging from 6.2 kg/mol to 2.8 kg/mol (Table **S1**).

Table 1. Polymer Yields/Conversions, Molecular Weights, *Đ*, Dyad Isotacticity and SCLC mobilities for family of isotactic PCzXA polymers with different alkyl chain spacers.

Polymer	Carbon Spacer	Yield[a]/Conversion[b] (%)	M_n (kg/mol)	*Đ*	Dyad Tacticity[e]	μ_h ($cm^2V^{-1}s^{-1}$)[f,h] Non - Annealed	μ_h ($cm^2V^{-1}s^{-1}$)[g,h] Annealed
9a	-	40[a]	33.4[c]	1.5	74.3	-	-
9b	-	45[a]	13.5[c]	2.0	86.7	-	-
10a	2	99[b]	24.9[d]	2.4	74.3	(3.0±0.22)x10^{-5}	(5.5±0.39)x10^{-5}
11a	4	98[b]	26.4[d]	2.8	74.3	(4.2±0.74)x10^{-5}	(7.2±0.27)x10^{-5}
12a	6	97[b]	27.2[d]	2.7	74.3	(2.9±0.45)x10^{-5}	(3.5±0.15)x10^{-5}
13a	8	98[b]	29.6[d]	2.4	74.3	(8.9±0.40)x10^{-6}	(1.4±0.09)x10^{-5}
14a	10	99[b]	31.7[d]	2.8	74.3	(5.5±0.18)x10^{-6}	(1.1±0.53)x10^{-5}
15a	12	98[b]	32.3[d]	2.1	74.3	(2.7±0.62)x10^{-6}	(9.1±0.57)x10^{-6}
10b	2	99[b]	21.4[d]	3.0	86.7	(4.5±0.41)x10^{-5}	(1.1±0.14)x10^{-4}
11b	4	97[b]	22.7[d]	2.7	86.7	(6.2±0.29)x10^{-5}	(1.5±0.35)x10^{-4}
12b	6	98[b]	24.3[d]	2.6	86.7	(7.4±0.44)x10^{-5}	(2.0±0.27)x10^{-4}
13b	8	98[b]	27.0[d]	2.2	86.7	(9.0±0.77)x10^{-6}	(9.7±0.62)x10^{-5}
14b	10	99[b]	27.8[d]	2.9	86.7	(5.2±0.35)x10^{-6}	(8.8±1.10)x10^{-5}
15b	12	98[b]	29.3[d]	2.4	86.7	(4.7±0.53)x10^{-6}	(7.5±0.47)x10^{-5}

[a]Polymerization yield, [b]Transesterification conversion, determined by ^{1}H NMR. [c]Determined by SEC with polystyrene standards and THF eluent. [d]Determined by SEC with polystyrene standards and *o*-DCB eluent. [e]Determined from ^{1}H NMR. [f]Measured from neat, as-cast polymer films. [g]Measured from polymer films after 30min annealing at 150 °C. [h]Data represents an average of at-least 12 pixels.

The observation of decreasing molecular weight as the spacer length increased is conjectured to be due to intramolecular interaction between the aromatic ring and the lithium counterion coordinated with the acrylate, which hinders chain propagation.

To target higher molecular weights and to have a more accurate comparison of spacer length, we moved to post-polymerization functionalization (**Scheme 1**), specifically taking inspiration from the transesterification of poly(methyl acrylate) (PMA) using ZnTac24 as catalyst.[42] Synthesis of **2** was achieved according to the literature.[46] Compounds **7b-7f**, were synthesized based on a literature procedure.[47] PMA was synthesized at two different levels of isotacticity. Polymer **9a** was synthesized using n-BuLi in toluene at -20 °C,[48] yielding dyad tacticity of 74.3% with an Mn of 33.4 kg/mol. Polymer **9b** was synthesized using PhMgBr in toluene at 0 °C [48] resulting in 86.7% dyad tacticity with an Mn of 13.5 kg/mol. The polymers were synthesized using standard Schlenk techniques and extraordinary measures commensurate with rigorous anionic polymerization were not applied for this model structure-function study as is consistent with the dispersities of 1.5 and 2.0. The difference in dyad isotacticity is due to stronger coordination of Mg^+ with the terminal and penultimate carbonyl oxygens as compared to Li^+, enforcing a higher percentage of meso placement.[49]

Scheme 1. Synthesis of monomers, PMA polymers, and PCzXA polymers.

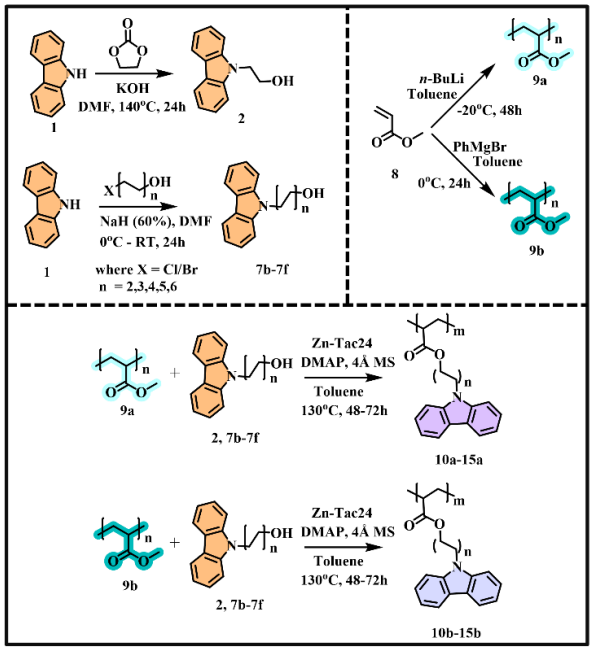

Polymers **9a** and **9b** were subjected to transesterification with compounds **2** and **7b-f** using ZnTac24.[50] Polymers **10a-15a** were derived from the lower tacticity **9a**, and polymers **10b-15b** were derived from the higher tacticity **9b**. All transesterifications proceeded with high conversions of >97%, as calculated from ^{1}H NMR (Table **1**). The lower tacticity polymers **10a-15a** were soluble in chloroform at 10 mg/ml and the solubility increased as the spacer length increased. The higher tacticity polymers **10b-15b** were only soluble after stirring at 60 °C in chloroform at 10 mg/ml with solubility also increasing as the spacer length increased. This method of post-polymerization functionalization promises a method to make new NCPEPs which would otherwise be inaccessible via direct anionic polymerization.

We used the space charge limited current (SCLC) technique to measure the hole mobilities of polymer thin films with and without annealing (Table **1** and Figure **2**). All the polymers were dissolved in chloroform, and then spin coated to yield films of thickness of 55nm - 65nm.

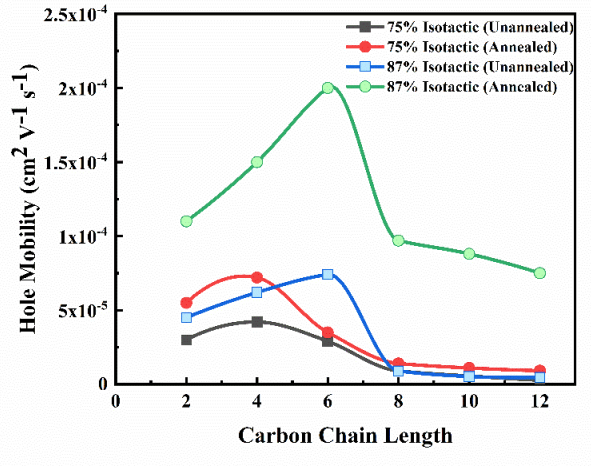

Figure 2. Relationship of hole mobility of as cast and annealed films for the polymers with different spacer chain lengths.

For the unannealed polymers with isotacticity of ~75% (**10a-15a**), as the spacer length increased from two carbons to four carbons, the μ_h increased from 3.0 x 10^{-5} cm^2 V^{-1} s^{-1} (**10a**) to 4.2 x 10^{-5} cm^2 V^{-1} s^{-1} (**11a**) and then gradually decreased with longer spacers to 2.7 x 10^{-6} cm^2 V^{-1} s^{-1} for the twelve-carbon spacer (**15a**). Even though the μ_h decreases after four carbons, there is little change cross the longer spacers (8-12 carbons). The effect of alkyl spacer length was similar for the unannealed polymers with ~87% isotacticity (**10b-15b**). However, in this case, the μ_h peaks with the six-carbon spacer. Hence the μ_h increases from 4.5 x 10^{-5} cm^2 V^{-1} s^{-1} for the two-carbon spacer (**10b**) to 7.4 x 10^{-5} cm^2 V^{-1} s^{-1} for six-carbon spacer (**12b**) and then sharply drops to 9 x 10^{-6} cm^2 V^{-1} s^{-1} for the eight-carbon spacer (**13b**) and gradually decreases thereafter. Based on the results of the unannealed films, the optimal spacer length for high μ_h is based on the degree of isotacticity, which show that the influence of isotacticity and spacer length are not independent.

Similar trends were observed for the annealed films but with higher values for μ_h. The annealing conditions were not optimized and our previously reported conditions for PCzEA of 150 °C for 30 mins were used. With the 75% isotactic polymers, the trend was the same before and after annealing, but the annealed samples with two and four-carbon spacers showed slightly higher mobilities. For spacer lengths of six to twelve carbons there was almost no change induced by annealing.

For the 87% isotactic polymers, annealing did not change the trend, but did result in dramatic increases in mobility for all samples. Specifically, a μ_h of 1.1 x 10^{-4} cm^2 V^{-1} s^{-1} was measured for the two-carbon spacer (**10b**), which increased to 2 x 10^{-4} cm^2 V^{-1} s^{-1} for six carbons (**12b**) (competitive with most conjugated polymers known in literature[51]) and then sharply drops down to 9.7 x 10^{-5} cm^2 V^{-1} s^{-1} for the eight-carbon spacer (**13b**) and further gradually decreases. Even though μ_h of the annealed six-carbon spacer (**12b**) reached 2.0 x 10^{-4} cm^2 V^{-1} s^{-1}, it still falls short of our previously reported μ_h for the annealed ~95% isotactic PCzEA, which suggests that even higher μ_h can be achieved with higher control over tacticity.

To gain insight into the mobility-spacer length-tacticity relationship we sought to look beyond primary structure correlations. As a first step we investigated thin film UV-Vis absorption which was found to be mostly invariant but we observed a slight blue shift (supporting information) in the case of the two-carbon spacer for both levels of tacticity indicating the possibility of H-aggregation with the two-carbon spacer.[52] For all films characteristic carbazole π-π^* transitions (~295 nm) and n-π^* transitions (~330 nm and 344 nm) were observed. Similarly, the HOMO levels of all the polymers were found to be the same as measured by cyclic voltammetry (5.82 - 5.86 eV).

Photoluminescence (PL) spectra yielded some structural insight (Supporting Information). In general, 0-0 transitions were observed at 350 nm with another vibronic band at 368 nm. Sharper peaks were observed from 405 to 430 nm corresponding to excimer emission, which is diagnostic of π-stacking.[53] For the 75% isotactic polymers (**10a-15a**), with spacers longer than four carbons, the excimer emission peaks are no longer prominent. A similar trend is also observed for the 87% isotactic polymers (**10b-15b**), where with spacers longer than eight carbons, the excimer peaks are not as sharp. It can be inferred that with polymers of lower isotacticity, π-stacking is more favorable only at shorter spacer lengths. This corresponds well with the hole mobility data. With higher isotacticity, π-stacking remains favorable to longer spacer lengths, which is again consistent with the mobility data.

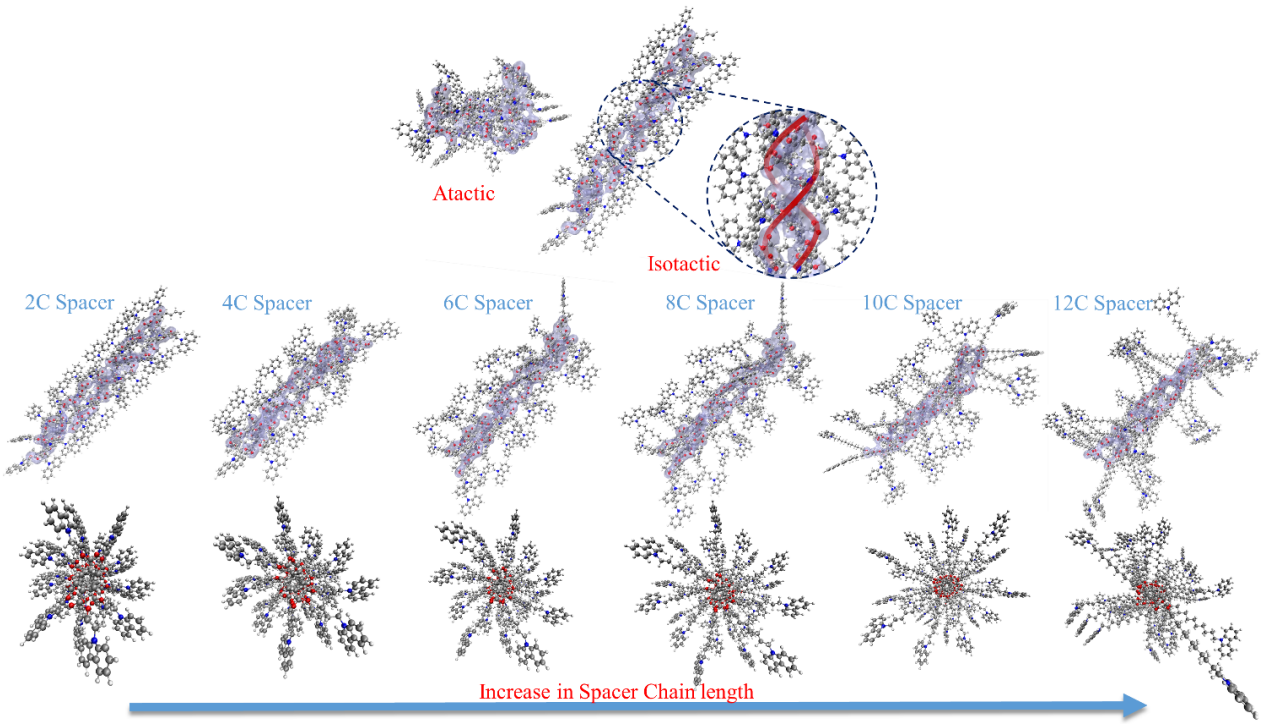

Figure 3. DFT optimized structures of atactic PCzEA and isotactic PCzEA (with inset showing helical backbone) (top) and isotactic polymer chains of PCzXA with increasing spacer chain length (bottom). The polymer backbones are highlighted and all polymers have 40 repeat units.

To study the morphology more directly, thin films were further analyzed by grazing incidence X-ray diffraction (GIXRD); however, no peaks were observed for any of the films, in agreement with what we had seen previously with PCzEA. The results from GIXRD are also consistent with DSC where no prominent peaks were observed for any samples (Supporting information). As such, these polymers appear to be largely amorphous and it is difficult to gain deep insight into the bulk structure and π-stacking.

We therefore elected to turn to simulations to model chain and bulk structure. A database of atactic and fully isotactic PCzXA chains with 20 and 40 monomers for each spacer length was generated. These chains were optimized using B3LYP/6-31+G(d) in Q-Chem 5.0.[54] From the DFT optimized structures (Figure **3**) with 40 repeating units, there is clearly a significant difference between the atactic and isotactic structures. Where the atactic structure is more randomized and clumped, the isotactic structures are elongated with all the pendant units surrounding the helical backbone. As the spacer is increased from two to twelve carbons for the isotactic polymers, the orientation of pendant units becomes more disorganized and tends toward π-stacked dimers even though the backbone remains helical. This type of helical structure is seen in many isotactic polymers.[55,56] Looking down the axis of the polymer chains, we see that the carbazoles are nicely oriented around the backbone with the four-carbon and six-carbon spacers, as opposed to the two-carbon spacer, which is more compact and slightly puckered. As the spacer length increases from eight carbons to twelve carbons, the favorable orientation is deviated and the pendant groups are more randomly organized.

To understand the effect of annealing and how the polymers pack in a thin film, we turned to MD simulations (Figure **4**). The initial topology files for 20 monomer chains (MD calculations used 20 monomers because of computational limitations) were obtained from Automated Topology Builder (ATB) and Repository (Version 3.0).[57] Chains of each polymer were permitted to relax for 1ns in isolation at 300K (using the LAMMPS suite), according to the intramolecular components of the GROMOS_54A7 force field, thus mimicking their arrangement in solution. A total of 64 relaxed chains for each polymer were placed in a bounded simulation box at periodic positions and orientations, with sufficient space between chains to avoid interchain interactions. This simulation volume was then compressed over a period of 40 ps at 300K until the density reached an average of 1.2 g/ml (density of PVK)[58], mimicking the effect of solvent evaporation. The morphologies were simulated with varying temperature from 300K to 425K for 4ns. The annealed films were finally cooled down to room temperature over a further 4ns period, before equilibrating at 300K for a final of 4ns. **Figure 4a** illustrates the case of the six-carbon spacer (detailed calculation steps for all spacers are in the supporting information).

From these MD simulations, it was observed that as the films were annealed, the interactions between chains increases significantly. Upon mapping the carbazole moieties, we see an enhanced π-π stacked short range ordering between multiple chains (**Figure 4b**) and the highest interchain π-π stacking is observed for the six-carbon spacer. These simulated results with 100% isotactic polymer help to explain why the 87% isotactic polymer shows the highest mobility with a six-carbon spacer. However, the 75% isotactic polymer shows the highest mobility with the four-carbon spacer. We propose that as the polymer becomes more atactic, that extended interchain interactions (to form continuous pi-stacked pathways) become less favorable in the more disordered system and intrachain interactions become more important to the overall mobility. We observe in the DFT models that the degree of intrachain ordering of the carbazole units increases as the spacer length decreases. As such, isotactic sequences based on shorter spacers are expected to give rise to more local (intrachain) ordering and dominate the mobility.

We notice that there is little difference between the mobility for the 2 and 4 carbon spacers in the case of the 75% isotactic sample (with and without annealing). We postulate that the 4-carbon spacer leads to a somewhat higher mobility than the 2-carbon spacer due to slightly enhanced intermolecular interactions that are favored with the longer spacer.

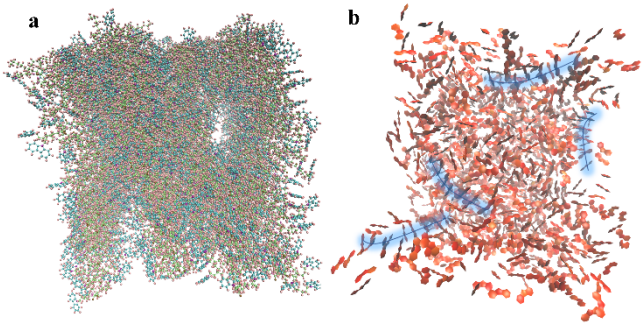

Figure 4. **a**) MD simulations of 64 chains of PCzHA (six-carbon spacer) packed into a thin film configuration after annealing. **b**) The stacking of different carbazole units from multiple chains showing short range ordering (blue labelling).

Here we have reported the effect of spacer lengths in NCPEPs on the charge carrier mobility in stereoregular polymers. Specifically, the hole mobility was observed to increase as the spacer length increases from two carbons to four carbons for the 75% isotactic polymer and up to a six-carbon spacer for the 87% isotactic polymer. With further increase in the spacer length, the hole mobility decreases rapidly and the effect of tacticity is diminished. It is found that this increase in hole mobility is likely due to a helical orientation in the isotactic polymers which increases the short range π-π stacked ordering in the thin films, especially with annealing, as simulated via DFT and MD. Considering the potential advantages of NCPEPs over CPs, these results show that NCPEPs can be designed to rival the mobility of conjugated polymers by tuning not only degree of isotacticty, but also the spacer length.

ASSOCIATED CONTENT

Supporting Information.

Syntheses of polymers; ^{1}H spectra; DSC, CV traces, Charge carrier mobilities (J-V) plots, and Absorption and emission profiles. DFT and MD simulations of polymers. This material is available free of charge via the Internet at http://pubs.acs.org.

AUTHOR INFORMATION

Corresponding Author

* E-mail: barrycth@usc.edu

Notes

The authors declare no competing financial interest.

ACKNOWLEDGMENT

We acknowledge funding from NSF-CBET (Energy for Sustainability (CBET-1803063)). S. S. also acknowledges funding from USC Dornsife (Dornsife Endowed Fellowship 2020 Award). We also acknowledge Dr. Marco Olguin at the USC Center for Advanced Research Computing for his insight and help in troubleshooting syntax errors for Molecular Dynamics Calculations.

REFERENCES

(1) Kim, M.; Ryu, S. U.; Park, S. A.; Choi, K.; Kim, T.; Chung, D.; Park, T. Donor–Acceptor-Conjugated Polymer for High-Performance Organic Field-Effect Transistors: A Progress Report. *Adv. Funct. Mater.* **2020**, *30* (20), 1–25. https://doi.org/10.1002/adfm.201904545.

(2) McBride, M.; Liu, A.; Reichmanis, E.; Grover, M. A. Toward Data-Enabled Process Optimization of Deformable Electronic Polymer-Based Devices. *Curr. Opin. Chem. Eng.* **2020**, *27*, 72–80. https://doi.org/10.1016/j.coche.2019.11.009.

(3) Sekine, C.; Tsubata, Y.; Yamada, T.; Kitano, M.; Doi, S. Recent Progress of High Performance Polymer OLED and OPV Materials for Organic Printed Electronics. *Sci. Technol. Adv. Mater.* **2014**, *15* (3), 034203. https://doi.org/10.1088/1468-6996/15/3/034203.

(4) Inganäs, O. Organic Photovoltaics over Three Decades. *Adv. Mater.* **2018**, *30* (35). https://doi.org/10.1002/adma.201800388.

(5) Sirringhaus, H. 25th Anniversary Article: Organic Field-Effect Transistors: The Path beyond Amorphous Silicon. *Adv. Mater.* **2014**, *26* (9), 1319–1335. https://doi.org/10.1002/adma.201304346.

(6) Lopez, J.; Mackanic, D. G.; Cui, Y.; Bao, Z. Designing Polymers for Advanced Battery Chemistries. *Nat. Rev. Mater.* **2019**, *4* (5), 312–330. https://doi.org/10.1038/s41578-019-0103-6.

(7) Fidanovski, K.; Mawad, D. Conjugated Polymers in Bioelectronics: Addressing the Interface Challenge. *Adv. Healthc. Mater.* **2019**, *8* (10), 1–9. https://doi.org/10.1002/adhm.201900053.

(8) Wang, Y. J.; Yu, G. Conjugated Polymers: From Synthesis, Transport Properties, to Device Applications. *J. Polym. Sci. Part B Polym. Phys.* **2019**, *57* (23), 1557–1558. https://doi.org/10.1002/polb.24911.

(9) Dou, K.; Wang, X.; Du, Z.; Jiang, H.; Li, F.; Sun, M.; Yang, R. Synergistic Effect of Side-Chain and Backbone Engineering in Thieno[2,3-f] Benzofuran-Based Conjugated Polymers for High Performance Non-Fullerene Organic Solar Cells. *J. Mater. Chem. A* **2019**, *7* (3), 958–964. https://doi.org/10.1039/c8ta07544a.

(10) Liu, K.; Jiang, Y.; Bao, Z.; Yan, X. Skin-Inspired Electronics Enabled by Supramolecular Polymeric Materials. *CCS Chem.* **2019**, *1* (4), 431–447. https://doi.org/10.31635/ccschem.019.20190048.

(11) Huang, J.; Chen, Z.; Mao, Z.; Gao, D.; Wei, C.; Lin, Z.; Li, H.; Wang, L.; Zhang, W.; Yu, G. Tuning Frontier Orbital Energetics of Azaisoindigo-Based Polymeric Semiconductors to Enhance the Charge-Transport Properties. *Adv. Electron. Mater.* **2017**, *3* (11), 1–8. https://doi.org/10.1002/aelm.201700078.

(12) Das, P.; Zayat, B.; Wei, Q.; Salamat, C. Z.; Magdău, I.-B.; Elizalde-Segovia, R.; Rawlings, D.; Lee, D.; Pace, G.; Irshad, A.; et al. Dihexyl-Substituted Poly(3,4-Propylenedioxythiophene) as a Dual Ionic and Electronic Conductive Cathode Binder for Lithium-Ion Batteries. *Chem. Mater.* **2020**, *32* (21), 9176–9189. https://doi.org/10.1021/acs.chemmater.0c02601.

(13) Jørgensen, M.; Norrman, K.; Gevorgyan, S. A.; Tromholt, T.; Andreasen, B.; Krebs, F. C. Stability of Polymer Solar Cells. *Adv. Mater.* **2012**, *24* (5), 580–612. https://doi.org/10.1002/adma.201104187.

(14) Root, S. E.; Savagatrup, S.; Printz, A. D.; Rodriquez, D.; Lipomi, D. J. Mechanical Properties of Organic Semiconductors for Stretchable, Highly Flexible, and Mechanically Robust Electronics. *Chem. Rev.* **2017**, *117* (9), 6467–6499. https://doi.org/10.1021/acs.chemrev.7b00003.

(15) Ding, Z.; Kettle, J.; Horie, M.; Chang, S. W.; Smith, G. C.; Shames, A. I.; Katz, E. A. Efficient Solar Cells Are More Stable: The Impact of Polymer Molecular Weight on Performance of Organic Photovoltaics. *J. Mater. Chem. A* **2016**, *4* (19), 7274–7280. https://doi.org/10.1039/C6TA00721J.

(16) Verheyen, L.; Leysen, P.; Van Den Eede, M.-P.; Ceunen, W.; Hardeman, T.; Koeckelberghs, G. Advances in the Controlled Polymerization of Conjugated Polymers. *Polymer* **2017**, *108*, 521–546. https://doi.org/10.1016/j.polymer.2016.09.085.

(17) Yokozawa, T.; Ohta, Y. Transformation of Step-Growth Polymerization into Living Chain-Growth Polymerization. *Chem. Rev.* **2016**, *116* (4), 1950–1958. https://doi.org/10.1021/acs.chemrev.5b00393.

(18) Seo, K.-B.; Lee, I.-H.; Lee, J.; Choi, I.; Choi, T.-L. A Rational Design of Highly Controlled Suzuki–Miyaura Catalyst-Transfer Polycondensation for Precision Synthesis of Polythiophenes and Their Block Copolymers: Marriage of Palladacycle Precatalysts with MIDA-

Boronates. *J. Am. Chem. Soc.* **2018**, *140* (12), 4335–4343. https://doi.org/10.1021/jacs.7b13701.

(19) Baker, M. A.; Tsai, C.-H.; Noonan, K. J. T. Diversifying Cross-Coupling Strategies, Catalysts and Monomers for the Controlled Synthesis of Conjugated Polymers. *Chem. - A Eur. J.* **2018**, *24* (50), 13078–13088. https://doi.org/10.1002/chem.201706102.

(20) Qiu, Z.; Hammer, B. A. G.; Müllen, K. Conjugated Polymers – Problems and Promises. *Prog. Polym. Sci.* **2020**, *100*. https://doi.org/10.1016/j.progpolymsci.2019.101179.

(21) Schroot, R.; Schlotthauer, T.; Dietzek, B.; Jäger, M.; Schubert, U. S. Extending Long-Lived Charge Separation Between Donor and Acceptor Blocks in Novel Copolymer Architectures Featuring a Sensitizer Core. *Chem. - A Eur. J.* **2017**, *23* (65), 16484–16490. https://doi.org/10.1002/chem.201704180.

(22) Gopinath, J.; Canjeevaram Balasubramanyam, R. K.; Santosh, V.; Swami, S. K.; Kishore Kumar, D.; Gupta, S. K.; Dutta, V.; Reddy, K. R.; Sadhu, V.; Sainath, A. V. S.; et al. Novel Anisotropic Ordered Polymeric Materials Based on Metallopolymer Precursors as Dye Sensitized Solar Cells. *Chem. Eng. J.* **2019**, *358* (October 2018), 1166–1175. https://doi.org/10.1016/j.cej.2018.10.090.

(23) Noirez, L.; Keller, P.; Cotton, J. P. On the Structure and the Chain Conformation of Side-Chain Liquid Crystal Polymers. *Liq. Cryst.* **1995**, *18* (1), 129–148. https://doi.org/10.1080/02678299508036602.

(24) Pugh, C.; Kiste, A. L. Molecular Engineering of Side-Chain Liquid Crystalline Polymers by Living Polymerizations. *Prog. Polym. Sci.* **1997**, *22* (4), 601–691. https://doi.org/10.1016/s0079-6700(97)00001-4.

(25) Ndaya, D.; Bosire, R.; Vaidya, S.; Kasi, R. M. Molecular Engineering of Stimuli-Responsive, Functional, Side-Chain Liquid Crystalline Copolymers: Synthesis, Properties and Applications. *Polym. Chem.* **2020**, *11* (37), 5937–5954. https://doi.org/10.1039/d0py00749h.

(26) Wen, Z.; Yang, K.; Raquez, J. M. A Review on Liquid Crystal Polymers in Free-Standing Reversible Shape Memory Materials. *Molecules* **2020**, *25* (5), 1–13. https://doi.org/10.3390/molecules25051241.

(27) Sommer, M.; Lindner, S. M.; Thelakkat, M. Microphase-Separated Donor-Acceptor Diblock Copolymers: Influence of HOMO Energy Levels and Morphology on Polymer Solar Cells. *Adv. Funct. Mater.* **2007**, *17* (9), 1493–1500. https://doi.org/10.1002/adfm.200600634.

(28) Lindner, S. M.; Hüttner, S.; Chiche, A.; Thelakkat, M.; Krausch, G. Charge Separation at Self-Assembled Nanostructured Bulk Interface in Block Copolymers. *Angew. Chemie - Int. Ed.* **2006**, *45* (20), 3364–3368. https://doi.org/10.1002/anie.200503958.

(29) Sommer, M.; Hüttner, S.; Wunder, S.; Thelakkat, M. Electron-Conducting Block Copolymers: Morphological, Optical, and Electronic Properties. *Adv. Mater.* **2008**, *20* (13), 2523–2527. https://doi.org/10.1002/adma.200703070.

(30) Ferenczi, T. A. M.; Müller, C.; Bradley, D. D. C.; Smith, P.; Nelson, J.; Stingelin, N. Organic Semiconductor:Insulator Polymer Ternary Blends for Photovoltaics. *Adv. Mater.* **2011**, *23* (35), 4093–4097. https://doi.org/10.1002/adma.201102100.

(31) Scaccabarozzi, A. D.; Stingelin, N. Semiconducting:Insulating Polymer Blends for Optoelectronic Applications - A Review of Recent Advances. *J. Mater. Chem. A* **2014**, *2* (28), 10818–10824. https://doi.org/10.1039/c4ta01065e.

(32) D'Angelo, P.; Barra, M.; Cassinese, A.; Maglione, M. G.; Vacca, P.; Minarini, C.; Rubino, A. Electrical Transport Properties Characterization of PVK (Poly N-Vinylcarbazole) for Electroluminescent Devices Applications. *Solid. State. Electron.* **2007**, *51* (1), 101–107. https://doi.org/10.1016/j.sse.2006.11.008.

(33) Uryu, T.; Ohkawa, H.; Oshima, R. Synthesis and High Hole Mobility of Isotactic Poly(2-N-Carbazolylethyl Acrylate). *Macromolecules* **1987**, *20* (4), 712–716. https://doi.org/10.1021/ma00170a002.

(34) Gallego, J.; Pérez-Foullerat, D.; Mendicuti, F.; Mattice, W. L. Configurations Conducive to the Formation of Intramolecular Excimers in Poly(N-Vinyl Carbazole) and Its Copolymers. *J. Polym. Sci. Part B Polym. Phys.* **2001**, *39* (12), 1272–1281. https://doi.org/10.1002/polb.1101.

(35) Karali, A.; Dais, P.; Mikros, E.; Heatley, F. Conformational Analysis of Poly(N -Vinylcarbazole) by NMR Spectroscopy and Molecular Modeling. *Macromolecules* **2001**, *34* (16), 5547–5554. https://doi.org/10.1021/ma010117n.

(36) Samal, S.; Thompson, B. C. Converging the Hole Mobility of Poly(2- N-Carbazoylethyl Acrylate) with Conjugated Polymers by Tuning Isotacticity. *ACS Macro Lett.* **2018**, *7* (10), 1161–1167. https://doi.org/10.1021/acsmacrolett.8b00595.

(37) Kim, W.; Nishikawa, Y.; Watanabe, H.; Kanazawa, A.; Aoshima, S.; Fujii, A.; Ozaki, M. Stereoregularity Effect on Hole Mobility in Poly(N-Vinylcarbazole) Thin Film Evaluated by MIS-CELIV Method. *Jpn. J. Appl. Phys.* **2020**, *59* (SD), 0–5. https://doi.org/10.7567/1347-4065/ab554f.

(38) Mehta, K.; Peeketi, A. R.; Liu, L.; Broer, D.; Onck, P.; Annabattula, R. K. Design and Applications of Light Responsive Liquid Crystal Polymer Thin Films. *Appl. Phys. Rev.* **2020**, *7* (4). https://doi.org/10.1063/5.0014619.

(39) Pereira, F. V.; Borsali, R.; Ritter, O. M. S.; Gonçalves, P. F.; Merlo, A. A.; Silveira, N. P. da. Structure-Property Relationships of Smectic Liquid Crystalline Polyacrylates as Revealed by SAXS. *J. Braz. Chem. Soc.* **2006**, *17* (2), 333–341. https://doi.org/10.1590/S0103-50532006000200017.

(40) Mehravar, E.; Iturrospe, A.; Arbe, A.; Asua, J. M.; Leiza, J. R. Phase Behavior of Side-Chain Liquid-Crystalline Polymers Containing Biphenyl Mesogens with Different Spacer Lengths Synthesized: Via Miniemulsion Polymerization. *Polym. Chem.* **2016**, *7* (29), 4736–4750. https://doi.org/10.1039/c6py00791k.

(41) Hirao, A.; Goseki, R.; Ishizone, T. Advances in Living Anionic Polymerization: From Functional Monomers, Polymerization Systems, to Macromolecular Architectures. *Macromolecules* **2014**, *47* (6), 1883–1905. https://doi.org/10.1021/ma401175m.

(42) Kim, J. G. Direct Transesterification of Poly (Methyl Acrylate) for Functional Polyacrylate Syntheses. **2017**, 2554–2560. https://doi.org/10.1002/pola.28659.

(43) Ito, D.; Ogura, Y.; Sawamoto, M.; Terashima, T. Acrylate-Selective Transesterification of Methacrylate/Acrylate Copolymers: Postfunctionalization with Common Acrylates and Alcohols. *ACS Macro Lett.* **2018**, *7* (8), 997–1002. https://doi.org/10.1021/acsmacrolett.8b00502.

(44) Easterling, C. P.; Kubo, T.; Orr, Z. M.; Fanucci, G. E.; Sumerlin, B. S. Synthetic Upcycling of Polyacrylates through Organocatalyzed Post-Polymerization Modification. **2017**, 1–23.

(45) Gulfidan, D.; Sefer, E.; Koyuncu, S.; Acar, M. H. Neutral State Colorless Electrochromic Polymer Networks: Spacer Effect on Electrochromic Performance. *Polymer* **2014**, *55* (23), 5998–6005. https://doi.org/10.1016/j.polymer.2014.09.041.

(46) Farah, A. A.; Pietro, W. J. Synthesis and Characterization of Multifunctional Polymers via Atom Transfer Radical Polymerization of N-(Ω′-Alkylcarbazolyl) Methacrylates Initiated by Ru(II) Polypyridyl Chromophores. *J. Polym. Sci. Part A Polym. Chem.* **2005**, *43* (23), 6057–6072. https://doi.org/10.1002/pola.21027.

(47) Dunkel, P.; Barosi, A.; Dhimane, H.; Maurel, F.; Dalko, P. I. Photoinduced Electron Transfer (PET)-Mediated Fragmentation of Picolinium-Derived Redox Probes. *Chem. - A Eur. J.* **2018**, *24* (49), 12920–12931. https://doi.org/10.1002/chem.201801684.

(48) Matsuzaki, K.; Uryu, T.; Ishida, A.; Ohki, T.; Takeuchi, M. Stereoregularity of Poly(Methyl Acrylate). *J. Polym. Sci. Part A-1 Polym. Chem.* **1967**, *5* (8), 2167–2177. https://doi.org/10.1002/pol.1967.150050832.

(49) Uryu, T.; Ohaku, K.-I.; Matsuzaki, K. Stereoregularity of Poly(Alkyl α-Chloroacrylates) and Mechanism of Isotactic Polymerization. *J. Polym. Sci. Polym. Chem. Ed.* **1974**, *12* (8), 1723–1734. https://doi.org/10.1002/pol.1974.170120812.

(50) Hayashi, Y.; Ohshima, T.; Fujii, Y.; Matsushima, Y.; Mashima, K. A Trifluoroacetic Acid Adduct of a Trifluoroacetate-Bridged M4-Oxo-Tetranuclear Zinc Cluster, Zn4(OCOCF 3)6O·CF3CO2H: Synthesis under Mild Conditions and Catalytic Transesterification and Oxazoline Formation. *Catal. Sci. Technol.* **2011**, *1* (2), 230–233. https://doi.org/10.1039/c0cy00048e.

(51) Yu, R.; Yao, H.; Cui, Y.; Hong, L.; He, C.; Hou, J. Improved Charge Transport and Reduced Nonradiative Energy Loss Enable Over 16% Efficiency in Ternary Polymer Solar Cells. *Adv. Mater.* **2019**, *31* (36), 1–8. https://doi.org/10.1002/adma.201902302.

(52) Bricks, J. L.; Slominskii, Y. L.; Panas, I. D.; Demchenko, A. P. Fluorescent J-Aggregates of Cyanine Dyes: Basic Research and Applications Review. *Methods Appl. Fluoresc.* **2018**, *6* (1). https://doi.org/10.1088/2050-6120/aa8d0d.

(53) Martins, T. D.; Weiss, R. G.; Atvars, T. D. Z. Synthesis and Photophysical Properties of a Poly(Methyl Methacrylate) Polymer with Carbazolyl Side Groups. *J. Braz. Chem. Soc.* **2008**, *19* (8), 1450–1461. https://doi.org/10.1590/S0103-50532008000800003.

(54) Shao, Y.; Gan, Z.; Epifanovsky, E.; Gilbert, A. T. B.; Wormit, M.; Kussmann, J.; Lange, A. W.; Behn, A.; Deng, J.; Feng, X.; et al. Advances in Molecular Quantum Chemistry Contained in the Q-Chem 4 Program Package. *Mol. Phys.* **2015**, *113* (2), 184–215. https://doi.org/10.1080/00268976.2014.952696.

(55) Li, X.; Wang, R.; Wu, C.; Chen, J.; Zhang, J.; Cui, D.; Wan, X. Effect of the Tactic Structure on the Chiroptical Properties of Helical Vinylbiphenyl Polymers. *Polym. Chem.* **2019**, *10* (28), 3887–3894. https://doi.org/10.1039/c9py00481e.

(56) Ishitake, K.; Satoh, K.; Kamigaito, M.; Okamoto, Y. Asymmetric Anionic Polymerization of Tris(Trimethylsilyl)Silyl Methacrylate: A Highly Isotactic Helical Chiral Polymer. *Polym. J.* **2013**, *45* (6), 676–680. https://doi.org/10.1038/pj.2012.178.

(57) Malde, A. K.; Zuo, L.; Breeze, M.; Stroet, M.; Poger, D.; Nair, P. C.; Oostenbrink, C.; Mark, A. E. An Automated Force Field Topology Builder (ATB) and Repository: Version 1.0. *J. Chem. Theory Comput.* **2011**, *7* (12), 4026–4037. https://doi.org/10.1021/ct200196m.

(58) Sigma Aldrich. Poly (9-vinylcarbazole) https://www.sigmaaldrich.com/MSDS/MSDS/DisplayMSDSPage.do?country=US&language=en&productNumber=182605&brand=ALDRICH&PageToGoToURL=https%3A%2F%2Fwww.sigmaaldrich.com%2Fcatalog%2Fproduct%2Faldrich%2F182605%3Flang%3Den (accessed Apr 6, 2021).

Insert Table of Contents artwork here